ELSEVIER

Carbon nanotubes induced crystallization of poly(ethylene terephthalate)

K. Anoop Anand [a], U.S. Agarwal [b,*], Rani Joseph [a]

[a] Department of Polymer Science and Rubber Technology, Cochin University of Science and Technology, Cochin 682 022, Kerala, India
[b] Reliance Technology Centre, B-4 MIDC Industrial Area, Patalganga 410 220, India

Abstract

We have investigated the crystallization characteristics of melt compounded nanocomposites of poly(ethylene terephthalate) (PET) and single walled carbon nanotubes (SWNTs). Differential scanning calorimetry studies showed that SWNTs at weight fractions as low as 0.03 wt% enhance the rate of crystallization in PET, as the cooling nanocomposite melt crystallizes at a temperature 10 °C higher as compared to neat PET. Isothermal crystallization studies also revealed that SWNTs significantly accelerate the crystallization process. WAXD showed oriented crystallization of PET induced by oriented SWNTs in a randomized PET melt, indicating the role of SWNTs as nucleating sites.
© 2006 Elsevier Ltd. All rights reserved.

Keywords: Poly(ethylene terephthalate); Single walled carbon nanotubes; Crystallization

1. Introduction

Poly(ethylene terephthalate) (PET) is one of the most extensively used thermoplastic polyesters, which has assumed a role of primacy in fibres, films, packaging and molding materials [1–3]. Due to its performance characteristics such as hardness, clarity, wear-resistance, dimensional stability, resistance to chemicals, etc. PET has worldwide consumption next only to polyolefines. As compared to poly(butylene terephthalate) (PBT), the slower crystallization of PET limits its usage in engineering applications which require fast crystallization for low cycle time for injection molding. Enhancement of crystallization rate of PET is generally achieved through the addition of minerals such as talc or organic acid salts such as sodium benzoate. Other nucleating agents that have been mentioned in the literature include metal oxides and hydrides, residual catalysts and diamide segments [4–6]. Several workers have reported the use of nanoparticles, such as organically modified nanoclays as crystallization promoters for a variety of polymers [7,8]. This has prompted the evaluation of nanoclays for crystallization enhancement in PET also [9]. Carbon nanotubes [10,11], which can be considered as thin long cylinders made up by rolling graphite sheets, have been evaluated in recent years as additives to polymers for imparting several properties such as mechanical reinforcement, electrical and thermal conductivity, as well as faster crystallization. For example, Probst et al. found that carbon nanotubes can nucleate crystallization of poly(vinyl alcohol) at concentrations as low as 0.1 wt% [12]. The crystallization behaviour of polypropylene (PP) in the presence of single walled carbon nanotubes (SWNTs) has also been reported [13–15]. Nogales et al. recently found that SWNTs did not influence the crystal structure of PBT [16], but they did not evaluate the influence on crystallization rate. To our knowledge, there has been no report in literature that addresses the effect of carbon nanotubes on the rate of PET crystallization. We here investigate this through differential scanning calorimetry in transient and isothermal modes, carried out on nanocomposite samples of PET, melt compounded with SWNTs at concentrations of 0–3 wt%. Wide angle X-ray diffraction (WAXD) is used to demonstrate the orientation of crystallizing PET chains along SWNTs.

2. Experimental

2.1. Materials

Poly(ethylene terephthalate) pellets (characteristic cylindrical diameter ≈ 2.5 mm, length ≈ 3 mm) were obtained from Acordis Research (Arnhem, The Netherlands). The intrinsic viscosity of the polymer was determined to be 0.98 dL/g in 1/1 phenol/1,1,2,2-tetrachloroethane at 30 °C. SWNTs were purchased from CarboLex Inc., (Lexington, USA). They were prepared by arc discharge method and the average diameter of

* Corresponding author. Tel.: +91 9324542566; fax: +91 2192307799.
E-mail address: uday.agarwal@ril.com (U.S. Agarwal).

an individual tube was 1.4 nm and length in the range of 2–5 μm. The purity of as-prepared grade of SWNTs was 50–70%.

2.2. Preparation of PET–SWNT nanocomposites

A simple melt-compounding route was adopted for the preparation of PET/SWNT nanocomposites. The polymer and the SWNTs were vacuum dried at 150 °C for 12 h to avoid moisture induced degradation phenomena. The melt compounding was performed using a laboratory scale (60 cm³) Haake kneader (model-HBI System-90) operating at 40 rpm for 4 min at 270 °C. Nanocomposites at different concentrations (0.0–3.0 wt%) of SWNTs were prepared.

2.3. Intrinsic viscosity measurements

Relative viscosities (η_{rel}) of ($c = 0.5$ g/dL) solutions of PET or PET–SWNT samples in 1/1 mixture of phenol and 1,1,2,2-tetrachloroethane were determined using a Schott–Gerate viscometer at a constant temperature of 30 °C. The solutions were prepared by dissolving the polymer samples at 70 °C in the solvent, which is pre-dried with regenerated molecular sieves. They were filtered prior to the measurements so that the presence of small amounts of insoluble components from SWNTs in the nanocomposite samples did not affect the measurements. The IV values were calculated using a single point determination method [17,18] according to the relation:

$$IV = (1/c)[2(\eta_{rel} - 1) - 2\ln(\eta_{rel})]^{1/2} \qquad (1)$$

2.4. Differential scanning calorimetry (DSC)

Differential scanning calorimetry (DSC Q-100, TA Instruments) was employed to study the crystallization characteristics of the nanocomposites. Indium was used for temperature calibration ($T_m = 156.6$ °C, $\Delta H_m = 28.4$ J/g). All the samples were dried prior to the measurements and analyses were done in a nitrogen atmosphere using standard aluminum pans. Calorimetric measurements were done while the samples (4–5 mg) were exposed to the following temperature scans: heating at a rate of 20 °C/min to 310 °C, holding for 10 min to erase thermal history effects and then cooling to 50 °C at a rate of 20 °C/min during which the peak of crystallization exotherm was taken as the crystallization temperature, T_c. For analysis of the isothermal

crystallization characteristics, the samples were subsequently reheated to 310 °C at a rate of 20 °C/min, held at 310 °C for 2 min, and then cooled rapidly (60 °C/min) to the desired temperature for isothermal crystallization (210, 215, 220 or 225 °C). The heat of fusion (ΔH_m) and the heat of crystallization (ΔH_c) were determined from the areas of the melting and crystallization peaks, respectively.

2.5. Wide angle X-ray diffraction (WAXD)

The wide-angle X-ray diffraction (WAXD) measurements were carried out with a Rigaku X-ray generator, using Ni filtered Cu K$_\alpha$ radiation ($\lambda = 0.154$ nm) at 40 kV and 30 mA. The sample-to-film distance was 70 mm. The film was exposed for 3 h to the X-ray beam from a pinhole collimator with a diameter of 0.4 mm. Photographs were taken using a flat film camera.

3. Results and discussion

3.1. Crystallization characteristics

Considering the known strong dependence of the PET crystallization rate on its molecular weight, an evaluation of the effect of SWNTs on PET crystallization requires comparison at similar molecular weights. For this purpose, neat PET was also subjected to melt compounding under identical conditions as that for the PET–SWNT nanocomposite preparation, and hereafter called the 0 wt% (SWNT concentration) sample. The decline in molecular weight of PET as a result of thermal/hydrolytic/oxidative degradation during melt processing was monitored by intrinsic viscosity (IV) measurements. It was observed that the IV of PET drops from 0.98 to 0.88 dL/g during melt compounding (Table 1). The reported IV values in Table 1 are the average of at least five concordant measurements. Since all the samples had comparable IV (or molecular weight) after processing under identical conditions, we infer that we have reasonably eliminated the possible dependence of our crystallization measurements on the molecular weights of the samples.

The effect of SWNTs on the crystallization characteristics of melt compounded PET–SWNT nanocomposite samples was analyzed first with non-isothermal DSC experiments. The crystallization temperatures (T_c), the apparent melting temperatures (T_m) and the corresponding enthalpies (ΔH_c and ΔH_m) are also reported in Table 1.

Table 1
DSC-determined thermal characteristics of PET–SWNT nanocomposite samples

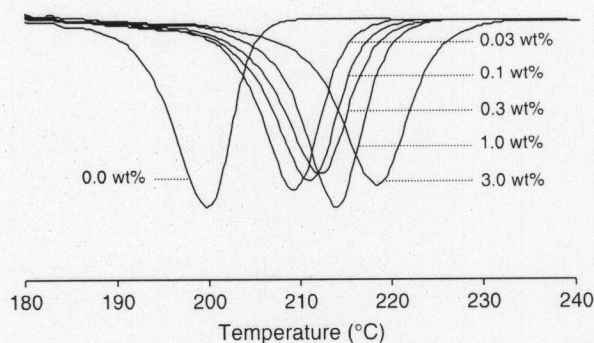| Concentration of SWNTs (wt%)	IV (dL/g)	T_c (°C)	ΔH_c (J/g)	T_m (°C)	ΔH_m (J/g)
0.0	0.884	199.9	38.2	253.0	36.5
0.03	0.878	209.9	37.5	251.7	37.8
0.1	0.881	211.5	36.6	252.5	36.2
0.3	0.875	212.4	37.6	253.5	37.3
1.0	0.883	214.3	37.2	251.1	37.7
3.0	0.879	219.1	36.8	252.5	38.8

Fig. 1. DSC cooling scans (20 °C/min from 310 °C melt) of PET–SWNT nanocomposite samples.

Fig. 1 shows the DSC cooling scans of PET–SWNT nanocomposite samples. During cooling from the melt, the SWNT containing samples show crystallization exotherms earlier than neat PET, as also seen from the corresponding T_c values indicated in Table 1. It is found that the nanocomposite sample containing SWNTs at a concentration as low as 0.03 wt% crystallizes 10 °C earlier than neat PET. The T_c values continue to increase with increasing SWNT concentration, but at a slower rate, as with the further 100 fold increase in SWNT concentration from 0.03 to 3.0 wt%, the additional T_c increase is only about 10 °C. In other words, there is a saturation of the nucleant effect at low SWNT concentrations, resulting in diminishing dependence on the increasing SWNT induced nucleation, possibly because of the large surface area and good dispersion of SWNTs. The

melting temperature and enthalpies of PET stay unaffected by SWNTs.

3.2. Isothermal crystallization characteristics

Fig. 2 shows the typical isothermal crystallization curves of the PET–SWNT nanocomposite samples at four temperatures (210, 215, 220 and 225 °C). The time corresponding to the maximum in the heat flow rate (exotherm) was taken as peak time of crystallization (t_{peak}). Such peaks are seen at each of the four isothermal crystallization temperatures for the 0.03 wt% SWNT containing nanocomposite, with the earlier or faster crystallization (smaller t_{peak}) corresponding to lower temperature of isothermal crystallization. For the case of neat PET, no
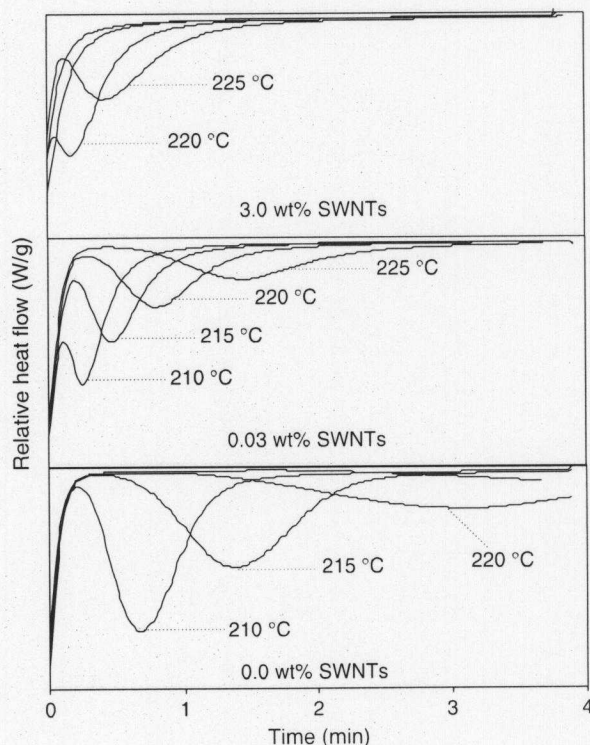

Fig. 2. Heat flow during isothermal crystallization of PET–SWNT nanocomposite samples.
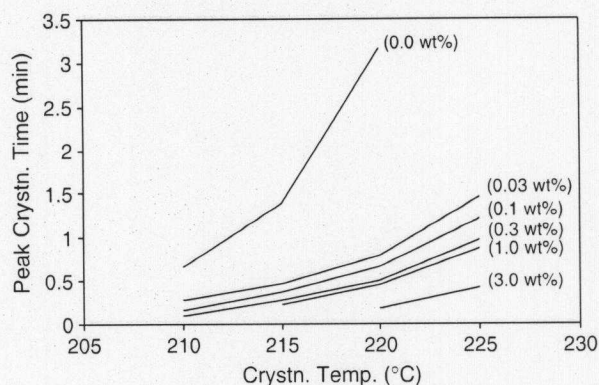
Fig. 3. Effect of SWNT concentration on the peak crystallization time of the nanocomposites at different isothermal crystallization temperatures.

peak is seen at the highest temperature of 225 °C because crystallization is very slow and would require longer time than the 4 min employed in our DSC program. On the other hand, for the nanocomposite sample with 3.0 wt% SWNTs, the rate of crystallization is so fast near the lowest temperatures (210 and 215 °C) that most crystallization occurs already during the cooling scan (60 °C/min) employed to reach those temperatures, resulting in absence of exothermic peaks in the heat flow curves at those temperatures.
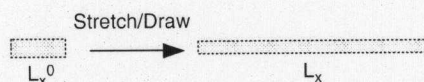
The peak times of crystallization at each of the temperatures for all the PET–SWNT nanocomposite samples are plotted against the isothermal crystallization temperature (Fig. 3). We notice that the t_{peak} values for the nanocomposite samples reduce to less than 50% as compared to neat PET due to the presence of SWNTs at concentrations as low as 0.03 wt%. With the increasing SWNT concentration there is further increase in the crystallization rate (as indicated by decrease in t_{peak}), demonstrating the role of SWNTs in enhancing the rate of crystallization.

3.3. SWNT-induced oriented crystallization

Wide-angle X-ray diffraction (WAXD) experiments provide opportunity to simultaneously analyze the crystalline structure, the extent of crystallization, as well as the crystalline orientation. This, combined with the rod like nature (large aspect ratio) of SWNTs, resulting in their easy orientation and difficult relaxation in highly viscous melts, offers an interesting possibility of directly verifying the role of SWNTs as nucleating sites for crystallization of the matrix polymer. Macroscopic orientation of SWNTs in relaxed PET was created by first stretching the solid nanocomposite sample under mechanical stress to orient

both SWNTs and the matrix polymer [19], followed by orientational relaxation of the matrix polymer alone. We compression molded neat PET and the PET–SWNT 1 wt% sample into 0.5 mm thick, 4 mm wide strips, and stretched these ($L_x/L_x^0 = 4$) times while heating in contact with a stainless steel plate at 150 °C (Scheme 1).

Fig. 4(A) and (C) show the oriented PET crystal structure in the drawn PET–SWNT nanocomposite and neat PET samples. It is expected that orientation of the PET molecules be accompanied by the orientation of the rod like SWNTs embedded therein. The strips were then positioned on glass slides with their ends glued to the glass slides to resist future macroscopic deformation (shrinkage). Subsequent heating at 20 °C/min to 300 °C on a hot stage allowed microscopic visualization of the polymer melting under cross polars. During melting, it is to be expected that the polymer molecules lose their orientation and randomize, while the SWNTs may retain their orientation since their disorientation would demand the difficult rotation of the entire long rod like structure entangled with the polymer matrix [20]. Subsequent cooling at a slow rate of 10 °C/min on the microscope hot stage allowed observation of PET crystallization. WAXD patterns of the resulting PET–SWNT 1 wt% nanocomposite and neat PET samples, shown in Fig. 4(B) and (D), respectively, indicate that the PET–SWNT sample shows oriented crystallization along the original stretching direction, while crystalline orientation is random in the neat PET case as expected. We infer the PET crystalline orientation in Fig. 4(B) emerging from the randomly oriented quiescent melt to be a result of the oriented SWNTs therein being responsible as nucleating sites for the reorientation of the crystallizing PET molecules.

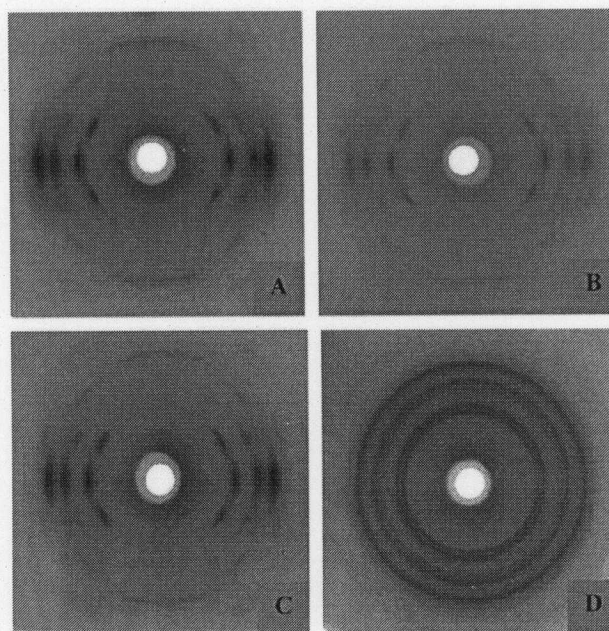Scheme 1. Stretching the solid nanocomposite sample to achieve orientation of the PET chains and SWNTs.

Fig. 4. WAXD patterns of the following samples: (A) PET/SWNT 1 wt% nanocomposite film after drawing, (B) PET/SWNT 1 wt% nanocomposite film after melting and subsequent slow cooling at constant length, (C) neat PET film after drawing, (D) neat PET film after melting and subsequent slow cooling at constant length. The drawing direction was vertical.

4. Conclusions

Melt compounded SWNTs have been shown to act as effective nucleating agents for PET crystallization. The SWNTs at a concentration as low as 300 ppm enhance the crystallization temperature during melt cooling by 10 °C, or reduce the melt's isothermal crystallization time by more than 50%. This, as well as the electrical conductivity threshold at 2 wt% concentration, and the accompanying increase in tensile and storage moduli (to be reported in a separate publication), indicate at a good dispersion of the SWNTs in the PET matrix. WAXD measurements indicate oriented crystallization of PET during cooling from randomised melts containing oriented SWNTs, supporting the hypothesis that the SWNTs induce crystallization of PET chains along the SWNTs.

Acknowledgements

References

[1] Paul DR, Barlow JW, Keskkula H. In: Mark HF, Bikales NM, Overberger ChG, Menges G, editors. Encyclopedia of polymer science and engineering, vol. 12. New York: Wiley; 1989.
[2] Fakirov S, editor. Handbook of thermoplastic polyesters. Weinheim: Wiley–VCH; 2002.
[3] Rieckmann Th, Volker S. In: Scheirs J, Long TE, editors. Modern polyesters. New York: Wiley; 2003.
[4] Van Bennekom ACM, Gaymans RJ. Polymer 1997;38:657.
[5] Bouma K, de Wit G, Lohmeijer JHGM, Gaymans RJ. Polymer 2000;41: 3965.
[6] Agarwal US, de Wit G, Lemstra PJ. Polymer 2002;43:5709.
[7] Ou CF. J Appl Polym Sci 2003;89:3315.
[8] Ou CF. J Polym Sci, Part B: Polym Phys 2003;41:2902.
[9] Ke Y, Long C, Qi Z. J Appl Polym Sci 1999;71:1139.
[10] Iijima S. Nature 1991;56:354.
[11] Ajayan PM. Chem Rev 1999;99:1787.
[12] Probst O, Moore EM, Resasco DE, Grady BP. Polymer 2004;45:4437.
[13] Grady BP, Pompeo F, Shambaugh RL, Resasco DE. J Phys Chem 2002;B-106:5852.
[14] Valentini L, Biagiotti J, Kenny JM, Santucci S. J Appl Polym Sci 2003; 87:708.
[15] Bhattacharyya AR, Sreekumar TV, Liu T, Kumar S, Ericson LM, Hauge RH, et al. Polymer 2003;44:2373.
[16] Nogales A, Broza G, Roslaniec Z, Schulte K, Sics I, Hsiao BS, et al. Macromolecules 2004;37:7669.
[17] Solomon OF, Ciuta IZ. J Appl Polym Sci 1962;6:683.
[18] Ma Y, Agarwal US, Sikkema DJ, Lemstra PJ. Polymer 2003;44:4085.
[19] Jin L, Bower C, Zhou O. Appl Phys Lett 1998;73:1197.
[20] Doi M, Edwards SF. The theory of polymer dynamics. New York: Oxford University Press; 1986.